

Symmetrical Switching of a Three-Phase Rectifier to improve the power factor in the mini hydroelectric frequency control

*L. A. Enríquez García¹, H. Bory², C. E. Mantilla¹, C. Miranda¹, C. Sánchez¹

¹ESPOCH, CEAA, Riobamba, Ecuador,

²Universidad de Oriente Sede Mella, Santiago de Cuba-Cuba,

¹ESPOCH, CEAA, Riobamba, Ecuador,

¹ESPOCH, CEAA, Riobamba, Ecuador,

¹ESPOCH, CEAA, Riobamba, Ecuador,

Corresponding Author: L. A. Enríquez García

Abstract: *this research analyzes a three-phase bridge rectifier, switches in series with the load switched symmetric angle, helping the effective current rates, active, reactive, apparent and distortion and power factor. The goal is to apply the switched rectifier with symmetrical angle for power factor improvement in micro hydroelectric power stations operating in isolated system, and changing the frequency regulating the power dissipated in the ballast loads alternating current AC converters. Interestingly, the power factor at the input terminals of the three-phase rectifier is slightly smaller than when converters CA-CA is used and despite this the rectifier improving the power factor of the network. In addition the power factor at the generator terminals in scheme uses the AC-AC converter is higher than in the converters and the load by separate users, this is because the active power consumed by users and by converters is greater than the total reactive power and distortion introduced by the converters. The three-phase rectifier bridge, with a series switch on the ballast switched symmetric angle load improves the power factor of the power system μ CH, a result corroborated by simulation and calculation, which is an improvement over the current circuit, AC-AC converter.*

Indexterms: *Rectifier; symmetrical switching; CA-CA converter; power factor; frequency control.*

Date of Submission: 02-08-2017

Date of acceptance: 17-08-2017

I. Introduction

At the present time there is a world-wide energetic crisis, where several countries have explored the renewable power sources. The hydraulic energy is one of the most important of them, which is improved by the construction of hydroelectric power-stations and small sized hydroelectric power-stations known as small, mini and micro hydroelectric to generate clean electricity (no fossil combustibles are used), therefore there is no poison gasses emitted to the atmosphere such as the Carbon Dioxide. Ecuador uses this technology where 16 hydroelectric power-stations are operating and are generating a power of 24 MW, located mainly in the central zone of the country and there are planned to install 10 mini hydroelectric power-stations more to increase the power electricity in 170 MW [1,2]. There is a project in Rwanda to Privately Develop Micro

Hydroelectric power-stations, in which four companies build, each one, power-plants from 100 to 150 kW to supply energy to a low voltage distribution net. [3]. In the article [4] is propose an advanced structure of a micro hydroelectric power-station based on a high speed turbine that is smaller, lighter, more efficient and stronger. The asset of the proposed design is that it is easiest and removes the mechanical adjustments trough a conditioning electronic power system to the connection to the electric network. The authors on [5] proposed a control structure that ensures the voltage and frequency regulation of an insulated induction generator. On [6] the authors report that in the United Kingdom there are small hydroelectric power-stations operating on 120 places producing a power of 100 MW with an unexplored potential of 400 MW. The articles [7], [8] and [9] are related to the costs analysis, the reckoning of the optimum installation capacity to the small hydroelectric power-stations according to technical, economical and reliability rates and the selection of small centrifuge pumps used as a turbine in micro hydroelectric power-stations respectively. On [10] the authors present the Power Electronics as the technology that brings the solution to problems that come from hydroelectric energy systems such as Networks integration, machinery control, frequency and voltage control and the power factor improvement. The authors on [11] present the hybrid control to the fitting of an integrated control system of optimization of coordination to coordinate the generation and the voltage automatic control system, which has always been considered they operate independently under the estimation of the active and reactive power control are disengaged. On [12] is proposed a model of the distributed generator vectorially controlled to a power flow based on the method of three-phase current injection. To obtain the model the output current per phase equations

are formulated on stationary state. The author of [13] presents an approximation to the frequency control of an interconnected power system using the theory of variable structure systems and the optimum control theory. A systematic procedure is developed to select the hyperplane commutation. The results obtained are based on simulation.

On [14] a simple mathematic algorithm is proposed to estimate the phase difference between the voltages and current that allows the calculation of power factor from electric power systems. The author asserts that the phase difference estimation with this algorithm is quick and is not affected when the current is distorted.

The articles commented on the previous paragraphs demonstrate the importance and the interest dedicated to the hydroelectric power sources from the scientist community.

This article will be focused on the small hydroelectric power-stations because they bring the electric service on intricate places without the need of big water reservoir or flows, producing a minor environment impact. In some of this micro hydroelectric power-plants (μ CHs), as there are not connected to the Electro energetic National System, the frequency control gets done by keeping constant the water flow and changing the dissipated power in a ballasted load connected in parallel with the users load, so that the Generation Power (PG), which is the one is trying to keep constant, is equal to the power dissipated on the o the ballasted load (PL) plus the power consumed by those users (PC) as is show on the Figure 1. Mathematically this is $PG = PL + PC$. [15, 16].

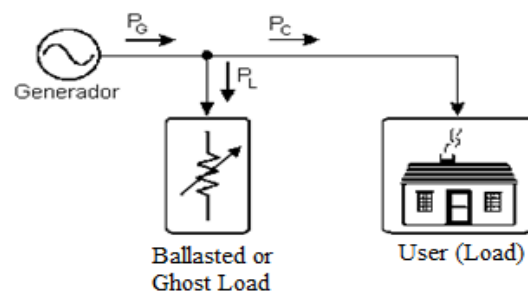


Figure 1. General working scheme of ballast frequency control.

The method of frequency control for ballasts loads using electronic controllers offer the following avails: more efficient regulation, the schemes of control are more robust, flexible and accurate; they do not present wastages, since there are no moving pieces neither they require the necessary maintenance of the mechanical-hydraulic regulators. [15, 16, 17].

Nowadays, as national as internationally, on the μ CHs that become frequency regulated by ballasts loads is use an Alternating Current-Alternating Current converter (AC-AC) to regulate the dissipated power on each ballast resistance. To set some examples it appears on the papers from Garcia in 2014 [18], from Abreu in 2006 [19], from Kurtz and Botteron [22], from Fong and et al in 2008 [23], from Hechavarria in 2008 [16], from Lee Dinh Suu in 2010 [24], from Suarez in 2010 [25], from Peña [26], from Vasquez [27] and from Bory in 2010 [28].

In the article by Kurtz and Botteron [22], the authors propose as an alternative to control the dissipated power in the ballast load, a three-phase bridge rectifier diode type (Graets bridge) with a power MOSFET, which acts as a switch in series with the load, which, in order to improve the power factor at its input, is switched by Pulse Width Modulation. This control has the disadvantage of using power devices of quick recovery that are more expensive and less available than devices of the same power but switched at low frequency.

In the articles [29] and [30] new forms of switching to different configurations of rectifier bridges with a resistive- inductive load, therein shows that depending on the way the components switch, the bridge can consume or provide reactive power or neither. The difficulty applying these methods has been the need to use multiple power devices (MCT, IGBT, GTO, etc...) that allow achieving these forms of commuting but are more expensive than the thyristors with the same power.

The purpose of this research is to switch with symmetric angle the rectifier proposed by Kurtz and Botteron [22], to improve the electrical system power factor of the micro hydroelectric power plants while controlling the dissipated power in the auxiliary load. The parameters to be analyzed are effective current, active, reactive, apparent and distortion power and power factor. The article presents the following structure: in section 1 introduction is performed; the section 2 titled Methodology is divided into the sections 2.1, in which a brief overview of the terms of the levels of performance and energy of the AC-AC converter is given and 2.2 in which is analyze the three-phase rectifier with a switcher in series with the load switched with symmetric angle obtaining the mathematical expressions of the performance and energy rates depending on the switching angle;

in section 3an application example to small hydroelectric power plants is develop where Three-phase rectifier and AC-AC converters are compared according to the mentioned rates and is proven the advantage of using the rectifier according to the power factor on the generator output; and Section 4, where the final conclusions of the article are given.

II. Methodology

A. Review on AC-AC converter

Below the mathematical expressions of the performance and energy parameters of the AC-AC converter previously mentioned are summarized. As the system analyzed has three phases there is a converter at each phase that regulates the amount of energy transferred from the alternator to the ballast loads, as well as considering that the converters are connected in star, are switched to the same angle shot, was use the four-wire connection, just analyzing one of the phases can get the results of the whole system. In Figure 2 the simulation scheme of the AC-AC converter for one phase is shown using the professional software Psim 6.0 [31].

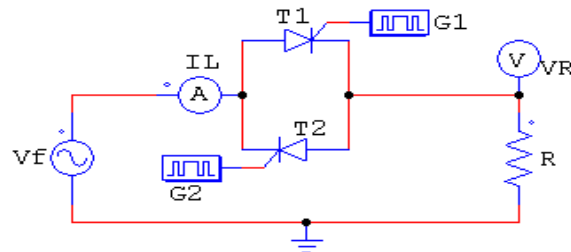


Figure 2. Simulation scheme of the AC-AC converter.

This simulation scheme presents: a sinusoidal voltage source (Vf) representing one phase of the alternator, with effective voltage (Veff) 110 V and frequency 60 Hz, the AC-AC converter formed by T1 and T2, two thyristors connected in antiparallel, the triggers (G1 and G2) whose function is to give the trigger pulse to the thyristors and its parameters are frequency (60 Hz), number of switching points (two) and switch points (the desired shooting angle shown), load resistance representing the ballast load in a phase (R = 4.03) and current and voltage markers (IL and VR) to display the waveforms of the converter input current and voltage in the load respectively.

The operation of the simulation scheme is as follows: for the positive half cycle of the input voltage T1 is triggered at angle after the zero crossing, causing it to pass to the conducting state allowing the power flow to pass from the source to the load. During the negative half cycle is triggered T2 at angle after zero crossing, causing it to pass to the conducting state allowing the power flow to pass from the source to the load. By changing the firing angle power flow is controlled. In Figure 3 the most significant waveforms of both voltage and current of the above circuit to an angle of 60° are shown to exemplify.

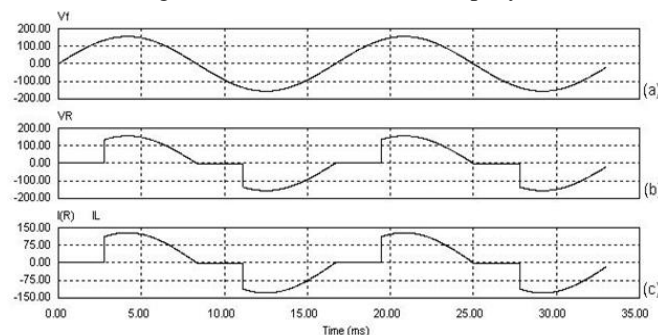


Figure 3. Most significant graphic wave forms from the AC-AC converter. (a) Voltage source, (b) voltage at the load, (c) current on the line the same load.

The effective value of the input Current is:

$$I_{rms} = \frac{V_{ef}}{R} \sqrt{\frac{1}{\pi} \left[\pi - \alpha + \frac{\sin(2\alpha)}{2} \right]} \quad (1)$$

The Active Power in the input to the AC-AC converter:

$$P_{inp} = \frac{V_{ef}^2}{\pi R} \left[\pi - \alpha + \frac{\text{sen}(2\alpha)}{2} \right] \quad (2)$$

When $\alpha = 0$, the Active Power reaches the maximum value $P_{\alpha 0} = \frac{V_{ef}^2}{R}$, which corresponds to the behavior of the converter, since for this α value, the source sees a pure resistance and this $P_{\alpha 0}$ is the power dissipated in this resistance. When $\alpha = \pi$, the input power reaches its minimum value, zero, since no power is transferred from the source to the load.

The reactive power at the input to the AC-AC converter:

$$Q_{inp} = \frac{V_{ef}^2}{\pi R} \left[\frac{1 - \cos(2\alpha)}{2} \right] \quad (3)$$

This power is positive, indicating that the network consumes it from the net. In Figure 4 the input reactive power divided between the maximum active power against power firing angle is plotted, it is zero for $\alpha = 0$, and $\alpha = \pi$. When $\alpha = \pi/2$ reactive power reaches its maximum value of 0.318 times the maximum active power, this is the maximum power consumption of the network. When $\alpha = 0$, reactive power is zero, since there is no phase difference between the fundamental component of the input current and the input phase voltage.

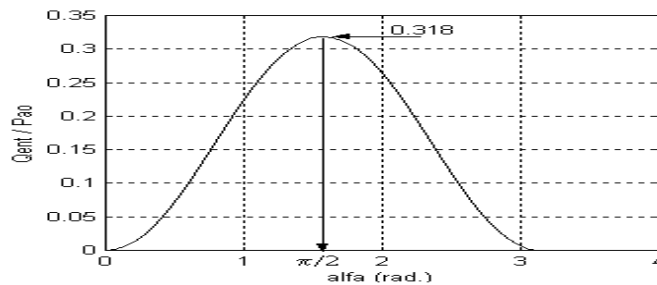


Figure 4. Graphical behavior of the relation $Q_{ent} / P_{\alpha 0}$ against the shooting angle.

An important aspect to mention is that each AC-AC converter, useful to control the power to be dissipated in a ballast resistor, consumes inductive reactive power contributing to worsen the power factor at the generator terminals.

The input apparent power to the AC-AC converter:

$$S_{inp} = \frac{V_{ef}^2}{R} \sqrt{\frac{1}{\pi} \left[\pi - \alpha - \frac{\text{sen}(2\alpha)}{2} \right]} \quad (4)$$

When $\alpha = 0$, apparent power has its maximum value, which is equal to the maximum active power dissipated in the load resistor. For $\alpha = \pi$, the source does not deliver power to the load so that the apparent power is zero, its lowest value.

The input distortion power to AC-AC Converter:

$$T_{inp} = \frac{\sqrt{2} V_{ef}^2}{2\pi R} \sqrt{2\alpha(\pi - \alpha) + (2\alpha - \pi)\text{sen}(2\alpha) + \cos(2\alpha) - 1} \quad (5)$$

For $\alpha = 0$, $T_{ent} = 0$ because the input current to the converter is not distorted. For $\alpha = \pi$ $T_{ent} = 0$, as the input current is zero.

For $\alpha = \pi/2$ distortion power reaches its maximum value of 0.386 times the maximum active power.

Now the power factor is determined:

$$f_p = \sqrt{\frac{1}{\pi} \left[\pi - \alpha + \frac{\sin(2\alpha)}{2} \right]} \quad (6)$$

For $\alpha = 0$ $f_p = 1$, because for this angle as the input current to the converter is perfectly sinusoidal and is in phase with the input voltage.

As the system is three-phase and therefore there is an AC-AC converter in each phase, which is supposed to commute with the same reference angle, the expressions of total power and power factor are:

- Three-phase active power P_{3inp}

$$P_{3inp} = 3P_{inp} = 3 \frac{V_{ef}^2}{\pi R} \sqrt{\frac{1}{\pi} \left[\pi - \alpha + \frac{\sin(2\alpha)}{2} \right]} \quad (7)$$

- Three-phase reactive power Q_{3inp}

$$Q_{3inp} = 3Q_{inp} = 3 \frac{V_{ef}^2}{\pi R} \left[\frac{1 - \cos(2\alpha)}{2} \right] \quad (8)$$

- Three-phase apparent power S_{3inp}

$$S_{3inp} = 3S_{inp} = 3 \frac{V_{ef}^2}{\pi R} \sqrt{\frac{1}{\pi} \left[\pi - \alpha + \frac{\sin(2\alpha)}{2} \right]} \quad (9)$$

- Three-phase power factor f_{p3}

$$f_{p3} = \frac{P_{3inp}}{S_{3inp}} = \sqrt{\left[\pi - \alpha + \frac{\sin(2\alpha)}{2} \right] \frac{1}{\pi}} \quad (10)$$

2.2. Analysis of the Bridge type three-phase rectifier with as switcher in series with the ballast loads witched with symmetrical angle.

Within this section is shown in Figure 5 the simulation scheme of three-phase rectifier with a switcher in series with the ballast or ghost load and the expressions of performance and energy rates previously mentioned according to the commutation angle are obtained.

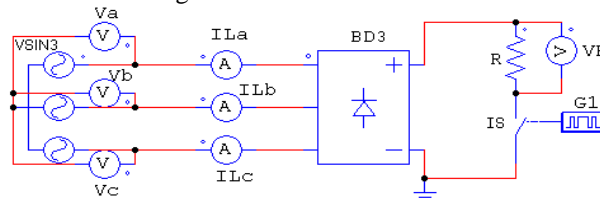


Figure 5. Simulation scheme of the three-phase rectifier with a switch in series with the ballast load.

The elements of the scheme are: three-phase sinusoidal voltage source (VSIN3) with 60Hz and a line voltage of 190.53V effective that represents the alternator; phase bridge rectifier diode (BD3), switch (SI) representing a switching component known as power bipolar transistor or IGBT; gating (G1) that represents the control unit, and its function is to apply a pulse to the switcher according to the switch form with symmetric angle and angle value desired, with switching frequency parameters (360Hz), number of switching points (2) and switch points (desired angle and width); load resistance (R), which represents the ballast load ($R = 4.03$) and markers of voltages and currents (Va, Vb, Vc, VR, ILA, ILB and ILC) displaying the wave forms of the phase voltages, the load voltage and line currents respectively. The scheme operates as follows: the diodes of the bridge lead up to 120° and switched every 60° , then to switch with a symmetric control angle, IS closes an angle α after the natural switching point and opens at the same α before next natural switching point, from this behavior can be state that the adjustment range is: $0 \leq \alpha \leq \pi/6$.

In Figure 6, the most significant wave forms of both voltage and current of the rectifier circuit for an angle equal to 150° are represented.

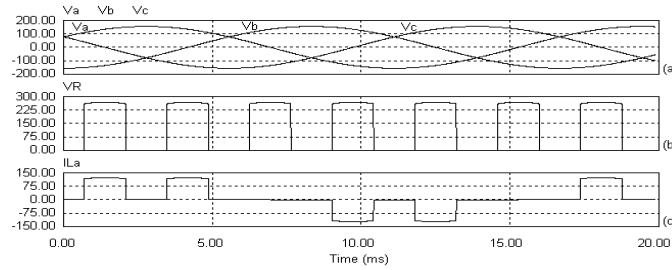


Figure 6. Graphics of the most significant waveforms of three-phase rectifier switched with symmetric angle. (a) Voltages of each phase of the source, (b) voltage at the load, (c) line current of phase A.

The wave form of the input current to the rectifier, as shown in Figure 6c for the phase **a**, has a period $T_{IL} = 2\pi$ whose analytical expression is given by Eq.(11).

$$i_L(\theta) = \left\{ \begin{array}{ll} 0 & \pi/6 < \theta < \pi/6 + \alpha \\ \frac{\sqrt{2}\sqrt{3}V_{ef}}{R} \text{sen}(\theta + \pi/6) & \pi/6 + \alpha < \theta < \pi/2 - \alpha \\ 0 & \pi/2 - \alpha < \theta < \pi/2 + \alpha \\ \frac{\sqrt{2}\sqrt{3}V_{ef}}{R} \text{sen}(\theta - \pi/6) & \pi/2 + \alpha < \theta < 5\pi/6 - \alpha \\ 0 & 5\pi/6 - \alpha < \theta < 7\pi/6 + \alpha \\ \frac{\sqrt{2}\sqrt{3}V_{ef}}{R} \text{sen}(\theta - 5\pi/6) & 7\pi/6 + \alpha < \theta < 3\pi/2 - \alpha \\ 0 & 3\pi/2 - \alpha < \theta < 3\pi/2 + \alpha \\ \frac{\sqrt{2}\sqrt{3}V_{ef}}{R} \text{sen}(\theta + 5\pi/6) & 3\pi/2 + \alpha < \theta < 11\pi/6 - \alpha \\ 0 & 11\pi/6 - \alpha < \theta < 2\pi + \pi/6 \end{array} \right\} \quad (11)$$

Then in Figure 6c shows that the converter input current per phase has odd symmetry and half-wave, which implies that: $a_0 = 0$, $a_n = 0$ for all n and $b_n = 0$ when n is pair. Since the coefficient a_1 is zero, the three-phase rectifier to the commutation switch tested does not consume or generate reactive power for any possible value of the power switching angle

Determining the coefficient b_1 :

$$b_1 = \frac{8}{T_{IL}} \int_0^{T_{IL}/4} i_L(\theta) \text{sen}(\theta) d\theta = \quad (12)$$

$$\frac{8}{2\pi} \int_{\pi/6+\alpha}^{\pi/2-\alpha} \frac{\sqrt{2}\sqrt{3}V_{ef}}{R} \text{sen}\left(\theta + \pi/6\right) \text{sen}(\theta) d\theta$$

$$b_1 = \frac{3\sqrt{2}V_{ef}}{\pi R} \left[\frac{\pi}{3} - 2\alpha + \frac{\sqrt{3}}{2} \cos(2\alpha) - \frac{\text{sen}(2\alpha)}{2} \right] \quad (13)$$

This coefficient indicates how much is the amplitude of the first harmonic of the current for each rectifier input terminal depending on the angle switching.

The effective value of the input current is:

$$I_{1rms} = \frac{3V_{ef}}{\pi R} \left[\frac{\pi}{3} - 2\alpha + \frac{\sqrt{3}}{2} \cos(2\alpha) - \frac{\text{sen}(2\alpha)}{2} \right] \quad (14)$$

For $\alpha = 0$, the effective value of the fundamental component of the input current to the converter reaches its maximum value:

$$I_{1rms\max} = \frac{3V_{ef}}{\pi R} \left[\frac{\pi}{3} + \frac{\sqrt{3}}{2} \right] \text{ and for } \alpha = \pi/6 \text{ it becomes zero, its lowest value.}$$

The offset angle ϕ_1 is zero for any value of the control angle, indicating that there is no phase difference between the phase voltage and the first harmonic of the input current to the rectifier, which corroborates the

stated above, the rectifier does not consume or generate reactive power. The displacement power factor is one

The effective value of the input current to the rectifier is:

$$I_{rms} = \sqrt{\frac{4}{T_{IL}} \int_0^{T_{IL}/4} [i_L(\theta)]^2 d\theta} = \sqrt{\frac{4}{2\pi} \int_{\pi/6+\alpha}^{\pi/2-\alpha} \left[\frac{\sqrt{2}\sqrt{3}V_{ef}}{R} \text{sen}(\theta + \pi/6) \right]^2 d\theta} \quad (15)$$

$$I_{rms} = \frac{\sqrt{2}\sqrt{3}V_{ef}}{R} \sqrt{\frac{1}{\pi} \left[\frac{\pi}{3} - 2\alpha + \frac{\sqrt{3}}{2} \cos(2\alpha) - \frac{\text{sen}(2\alpha)}{2} \right]} \quad (16)$$

Calculating the total active power at the rectifier input using the fundamental harmonic component of the input current in phase with the phase voltage.

$$P_{3inp} = 3V_{ef} \frac{b_1}{\sqrt{2}} \quad (17)$$

$$P_{3inp} = \frac{9\sqrt{6}V_{ef}^2}{\pi R} \sqrt{\left[\frac{\pi}{3} - 2\alpha + \frac{\sqrt{3}}{2} \cos(2\alpha) + \frac{\text{sen}(2\alpha)}{2} \right]} \quad (18)$$

For $\alpha = 0$ the total active power is maximum $P_{3inp \max} = \frac{9V_{ef}^2}{\pi R} \left[\frac{\pi}{3} + \frac{\sqrt{3}}{2} \right]$ and for $\alpha = \frac{\pi}{6}$ it is zero, the minimum value.

If set $P_0 = \frac{V_{ef}^2}{R}$ and divide the Eq. (18) for P_0 , is obtain the normalized expression of the total active power, in which the graph shown in Figure 7 an approximately linear behavior of this (compared with the reference line) is seen, thus making this switching rectifier with symmetric angle commutation in an ideal component of the control loop frequency.

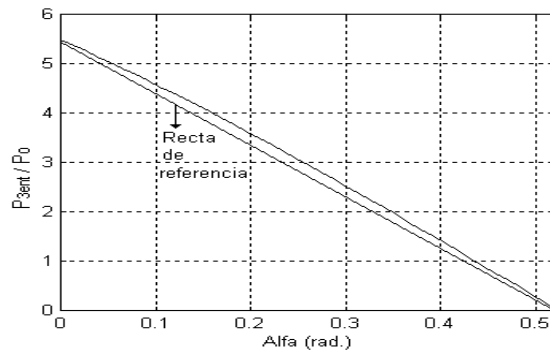


Figure 7. Graphical behavior of the relation P_{3ent}/P_0 against α .

The apparent total input power:

$$S_{3inp} = 3V_{rms}I_{rms} \quad (19)$$

$$S_{3inp} = \frac{3\sqrt{6}V_{ef}^2}{R} \sqrt{\frac{1}{\pi} \left[\frac{\pi}{3} - 2\alpha + \frac{\sqrt{3}}{2} \cos(2\alpha) + \frac{\text{sen}(2\alpha)}{2} \right]} \quad (20)$$

For $\alpha = 0$, the total apparent power to the rectifier input reaches its maximum value $S_{3inp \max} = \frac{3\sqrt{6}V_{ef}^2}{R} \sqrt{\frac{1}{\pi} \left[\frac{\pi}{3} + \frac{\sqrt{3}}{2} \right]}$. For $\alpha = \frac{\pi}{6}$, the three-phase apparent power is zero, its lowest value, since the source gives no power to the load. This power has an approximately parabolic curve as indicated by Eq. (20)

Phase distortion power is determined as:

$$T_{3inp} = \sqrt{S_{3inp}^2 - P_{3inp}^2} \quad (21)$$

$$T_{3inp} = \frac{9V_{ef}^2}{\pi R} \sqrt{\frac{\pi^2}{9} - \left[2\alpha - \frac{\sqrt{3}}{2} \cos(2\alpha) + \frac{\text{sen}(2\alpha)}{2} \right]^2} \quad (22)$$

For $\alpha = 0$ $T_{3inp} = 1.687 P_0$, nonzero value because the rectifier input current is distorted. For $\alpha = \frac{\pi}{6}$, $T_{3inp} = 0$, since the input current is zero.

Below the graphic of the total input distortion power split between P_0 against the angle α is shown, where is emphasized that for $\alpha = \frac{\pi}{12}$ this power reaches its maximum value of 2.999 times P_0

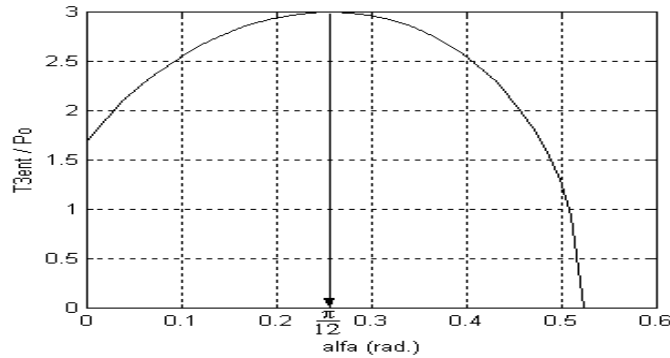


Figure 8. Graphic of T_{3ent} / P_0 against the commutation angle.

Then the power factor is determined:

$$f_p = \frac{P_{3inp}}{S_{3inp}} = \frac{\frac{9\sqrt{6}V_{ef}^2}{\pi R} \sqrt{\left[\frac{\pi}{3} - 2\alpha + \frac{\sqrt{3}}{2} \cos(2\alpha) + \frac{\sin(2\alpha)}{2}\right]}}{\frac{3\sqrt{6}V_{ef}^2}{R} \sqrt{\frac{1}{\pi} \left[\frac{\pi}{3} - 2\alpha + \frac{\sqrt{3}}{2} \cos(2\alpha) + \frac{\sin(2\alpha)}{2}\right]}} \quad (23)$$

$$f_p = \sqrt{\frac{3}{2\pi} \left[\frac{\pi}{3} - 2\alpha + \frac{\sqrt{3}}{2} \cos(2\alpha) - \frac{\sin(2\alpha)}{2} \right]} \quad (24)$$

It should be noted that for $\alpha = 0$ $f_p = 0.956$, because the input current to the rectifier for this angle is distorted. The power factor has an approximately parabolic curve as indicated by Eq. (24).

It is recalled that a total reactive power at the rectifier input is:

$$Q_{3inp} = 3V_{ef} \frac{a_1}{\sqrt{2}} = 0 \quad (25)$$

These results were expected and demonstrate that the rectifier that switches on the way previously described does not consume nor provides reactive energy to the net, which is considered as an improvement over the current use of the AC-AC converters, which consume reactive power contributing to worsen the power factor at the generator output

3.1. Application example of the rectifier.

In this section, an example is developed to illustrate the advantages of the three-phase rectifier switched with symmetrical angle versus AC-AC converter which is currently employed in the frequency control in a μ CH by ballast load. Suppose that after having a record of measurements of power, voltage and defective current in a μ CH, is known to have a low active power demanded by users, P_{UMIN} , is 3kW; the maximum active power demanded by users, P_{UMAX} , is 12kW and at a certain time the power demanded by users is $P_U = 7.5$ kW with a lag power factor $f_{pU} = 0.7$.

Example development—Considering that to control the power to be dissipated in the ballasts loads will be use a three-phase rectifier switched with symmetric angle is necessary to find the value of the ballast resistance, this value is calculated from the maximum active power should consume the three-phase rectifier, if is this: $P_{BD3máx} = P_{UMAX} - P_{UMIN} = 9$ kW, then evaluating equation (18) for $\alpha = 0$ has to be:

$$R_{ballast} = \frac{9V_{ef}^2}{\pi P_{BD3máx}} \left[\frac{\pi}{3} + \frac{\sqrt{3}}{2} \right] = 7.3689 \Omega \quad (26)$$

The chosen value of the ballast resistor is $R_{ballast} = 7.3 \Omega$, because it allows the frequency control when the power of the users is minimum.

The values of resistance and inductance per phase that represent the users load in ascertain in time of the day when they demand P_U with a power factor of 0.7 are: $R_U = 2.37 \Omega$ and $L_U = 6.418\text{mH}$ respectively. The total reactive power consumed by users and the effective current in each phase for these conditions are: $Q_U = 7.65\text{kVAR}$ and $I_U = 32.47\text{A}$.

In the time of the day that users consume the power P_U , the rectifier should be consuming an active power P_{BD3} of 4.5 kW and this is achieved with $\alpha = 0.282 \text{ rad}$ (16.16°).

For this α value and $R_{ballast}$, the effective current, power and power factor in the rectifier input are:

- The effective current eq. (16), $I_{BD3A} = I_{BD3B} = I_{BD3C} = 20.27 \text{ A}$.
- The total active power eq. (18) $P_{BD3} = 4.5006 \text{ kW}$.
- The total reactive power: $Q_{BD3} = 0 \text{ kVAR}$.
- The total apparent power eq. (20) $S_{BD3} = 6.690 \text{ kVA}$.
- The total power distortion eq. (22) $T_{BD3} = 4.950 \text{ kVAD}$.
- The power factor eq. (24): $fp_{BD3} = 0.6727$

In the generator terminals to the load conditions imposed by the users and the rectifier, the total active power (P_L), total reactive power (Q_L), total apparent power (S_L), total distortion power (T_L) and the factor power (fp_L) are:

- The total active power $P_L = 12.00 \text{ kW}$.
- The total reactive power $Q_L = 7.65 \text{ kVAR}$.
- Total Apparent Power: $S_L = 15.070 \text{ kVA}$.
- The total distortion power: $T_L = 4.950 \text{ kVAD}$.
- Power factor: $fp_L = 0.7966$.

Figure 9 shows the scheme used for the simulations in the professional software Psim 6.0[31].

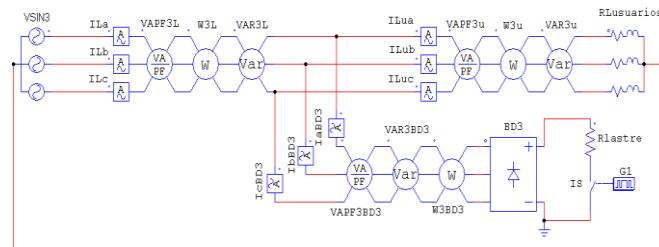


Figure 9. Simulation scheme with three-phase rectifier.

The elements of the scheme are: sinusoidal voltage source V_{SIN3} , which represents the alternator; users load, R_L users; the proposed three-phase rectifier consisting of $BD3$, IS and $G1$; the ballast load $R_{ballast}$; AC ammeters (I_{La} , I_{Lb} , I_{Lc} , I_{LuA} , I_{Lub} , I_{Luc} , I_{aBD3} , I_{bBD3} and I_{cBD3}) measuring the effective values in each phase of the current in the generator terminals, the load that represent the users and in the proposed rectifier respectively and the Watt meters, varmeters and apparent power and power factor meters ($W3L$, $VAR3L$, $VAPF3L$, $W3u$, $VAR3u$, $VAPF3u$, $W3BD3$, $VAR3BD3$ and $VAPF3BD3$) to measure the total power and power factor at the alternator output, at the users load and at the input of the rectifier bridge respectively. The simulation scheme representing the currently employed system differs from the one shown in Figure 9 on the replacement of the three-phase rectifier with three AC-AC converter, each connected between one phase and the neutral of the generator and that the names of the measuring instruments and therefore of the measured variables associated with these converters end with AC-AC. In the current scheme the three ballast resistors are $R_{ballast 1} = R_{ballast 2} = R_{ballast 3} = 4.03 \Omega$, one for each AC-AC converter. For these AC-AC converters consume 1.5kW must be switched at an angle of 90° , resulting in:

- Effective converter input current eq. (1), $I_{CACAC} = 19.30 \text{ A}$.
- Active power per phase, Eq. (2) $P_{fACAC} = 1.5 \text{ kW}$, total $P_{ACAC} = 4.5 \text{ kW}$.
- Reactive power per phase, Eq. (3) $Q_{fACAC} = 0.955 \text{ kVAR}$, total $Q_{ACAC} = 2.864 \text{ kVAR}$.
- Apparent power per phase, Eq. (4) $S_{fACAC} = 2,123 \text{ kVA}$, total $S_{ACAC} = 6,369 \text{ kVA}$.
- Power phase distortion, eq. (5) $T_{fACAC} = 1.157 \text{ kVAD}$, total $T_{ACAC} = 3.470 \text{ kVAD}$.
- The power factor of Eq. (6), $fp_{ACAC} = 0.7071$.

At the generator output, represented by V_{SIN3} , the active power is P_G (W), the reactive power is Q_G (kVAR), the apparent power S_G (VA), the distortion power (TG) and power factor (FPG).

- The total active power $P_G = 12.00 \text{ kW}$.
- The total reactive power: $Q_G = 10,514 \text{ kVAR}$.
- The total apparent power: $S_G = 16.331 \text{ kVA}$.

- The total distortion power: $T_G = 4.950$ kVAD.
 - Power factor: $fp_G = 0.735$.
- The Table 1 named Comparison between the simulation results of the three-phase rectifier switched with symmetric angle and the AC-AC converter shows the simulation results of both schemes.

TABLE I. Comparison between the simulation results of the three-phase rectifier switched with symmetric angle and the AC-AC converted

Variable	Three-phase Rectifier	AC-AC Converter
I _L a, I _L b, I _L c (generator output)	45.61 A	49.45 A
I _a BD3, I _b BD3, I _c BD3,	20.25 A	-
I _a CACA, I _b CACA, I _c CACA	-	19.27 A
W3L	12.002 kW	12.004 kW
VAR3L	7.656 kVAR	10.522 kVAR
VAPF3L (S)	15.065 kVA	16.323 kVA
VAPF3L, (fp)	0.7966	0.7354
W3BD3, W3CACA	4.501 kW	4.504 kW
VAR3BD3, VAR3CACA	-0.067 VAR	2.685 kVAR
VAPF3BD3, VAPF3CACA (S)	6.690 kVA	6.364 kVA
VAPF3BD3, VAPF3CACA, (fp)	0.6728	0.7077

From the results shown in Table 1, an excellent correspondence between calculated and simulated values is observed. From Table 1 is also noted that the reactive power value obtain by simulation for the scheme with the rectifier can be considered null due to its small size, this is the fundamental difference between the scheme employing the three-phase rectifiers witched with symmetric angle and the currently use scheme with AC-AC converters. The total reactive power consumed by the three AC-AC converters to control the angle of each converter of 90° represents a 37.4% of the total reactive consumed by users and a 27.23% of the total reactive power at the output of the generator.

Table 1 shows that the power factor at the terminal soft he source representing the alternator; eighth row (VAPF3L (fp)); for the scheme with three-phase rectifier switched with symmetric angle is greater than in the scheme with AC-AC converters, this is because he first does not consume reactive power, resulting in the decrease of the effective current in each phase of the alternator in approximately 4 A, as shown in the second row of Table 1, (I_La I_Lb, I_Lc(generator output)), increasing the availability of the alternator according to the delivery of active power, result that validates the circuit and the switching way proposed.

Interestingly, the power factor at the input terminals of the three-phase rectifier, according to calculations made and the last row of Table 1, is slightly smaller than when the AC-AC converters are used and despite this the rectifier improves the power factor of the network. It is also important to note that the power factor at the generator terminals in the scheme that uses the AC-AC converters is higher than in the converters and in the users load separately, this is due to the active power consumed by the converters and users is greater than total reactive power and distortion introduced by the converters.

III. Conclusion

The development of this research allowed obtaining the following conclusions:

The three-phase bridge rectifier in series with the ballast load switched with symmetric angle improves, or at least does not worsen, the power factor of the electrical system of the μCH, a result corroborated by simulation and calculation in the example discussed, which establishes an improvement over the existing circuit, the AC-AC converter. The three-phase rectifier increases the availability of a μCH electric generator over the existing circuit. Mathematical expressions of the performance and energy rates were obtained depending on the switching angle of the three-phase bridge rectifier with switcher in series with the resistive load, expressions that demonstrate that this switching does not provided or consumed reactive power. The AC-AC converters always consume reactive power except when the firing angle of the thyristors is 0° or 180°. The distortion power is zero for a firing angle of 0° in the AC-AC converter, while for the rectifier is approximately 1.7 times the maximum active power.

References

- [1] Hydroelectric. Available on line: https://www.google.com.ec/?gfe_rd=cr&ei=C652U6bQOM7AqAWoJYCQDA#q=total+centrales+hidroel%C3%A9ctricas+en+ecuator [Accessed: 15-01-2014].
- [2] Revistalideres.ec. Available on line: http://www.revistalideres.ec/informe-semanal/hidroelectricas-vienen-Ecuador energia_0_847115311.html [Accessed: 15-01-2014].
- [3] Maurice P, Robert J. "Innovative private micro-hydro power development in Rwanda". Available: <http://www.sciencedirect.com/science/article/pii/S0301421509004480> [Accessed: 20-04-2014].
- [4] Marquez JL, Molina MG, Pacas JM. "Dynamic modeling, simulation and control design of an advanced micro-hydro power plant for distributed generation applications". National University of San Juan, Argentina. Available: <http://www.sciencedirect.com/science/article/pii/S0360319910004003> [Accessed: 20-04-2014].
- [5] Ion C P, Marinescu C. "Autonomous micro hydro power plant with induction generator". Available: <http://www.sciencedirect.com/science/article/pii/S0960148111000504> [Accessed: 20-04-2014].
- [6] Paish O. "Small hydro power: technology and current status". Available on line: <http://www.sciencedirect.com/science/article/pii/S1364032102000060> [Accessed: 20-04-2014].
- [7] Aggidis G A, Luchinskaya E, Rothschild R, Howard DC. "The costs of small-scale hydro power production: Impact on the development of existing potential". Available: [http://www.researchgate.net/publication/222594079_The_costs_of_small scale_hydro_power_production_Impact_on_the_development_of_existing_potential](http://www.researchgate.net/publication/222594079_The_costs_of_small_scale_hydro_power_production_Impact_on_the_development_of_existing_potential) [Accessed: 15-04-2014].
- [8] Williams A. "Pumps as turbines for low cost micro hydro power". Available online: <http://www.sciencedirect.com/science/article/pii/S0960148196884989> [Accessed: 20-04-2014].
- [9] Hosseini S M H, Forouzabakhsh F, Rahimpour M. "Determination of the optimal installation capacity of small hydro-power plants through the use of technical, economic and reliability indices". Available online: <http://www.sciencedirect.com/science/article/pii/S0301421504000679> [Accessed: 21-04-2014].
- [10] Singh R R, Chelliah T Agarwal. "Power electronics in hydro electric energy systems – A review". Available on line: <http://www.sciencedirect.com/science/article/pii/S1364032114000525> [Accessed: 22-04-2014].
- [11] Lu Q, Hu W, Zheng L, Min Y, Li M, Li X, Ge W, Wang Z (2012). "Integrated Coordinated Optimization Control of Automatic Generation Control and Automatic Voltage Control in Regional Power Grids". Tsinghua University, China. Available online: <http://www.mdpi.com/1996-1073/5/10/3817> [Accessed: 23-04-2014].
- [12] Ik Hwang P, Moon Seung-II, JuAhn S. "A Vector-Controlled Distributed Generator Model for a Power Flow Based on a Three-Phase Current Injection Method". Chonnan National University. Available online: <http://www.mdpi.com/1996-1073/6/8/4269> [Accessed: 22-04-2014].
- [13] HsuYY "Optimal variable structure controller for the load-frequency control of interconnected hydrothermal power systems". National Taiwan University. Available on line: <http://www.sciencedirect.com/science/article/pii/S0142061584900048>. [Accessed: 24-04-2014].
- [14] Lütfü Sari bulut. "A simple power factor calculation for electrical power systems". Adana Science and Technology University, Turkey. Available on line: <http://www.sciencedirect.com/science/article/pii/S014206151400218X> [Accessed: 25-04-2014].
- [15] Mare J, Odello L (2001). "Regulators of intelligent frequency for micro hydro". National University of COMAHUE, Argentina.
- [16] Hechavarría M, Bell O (2008). "Frequency control in mini-hydroelectric isolated", Diploma Work. University of Oriente, Cuba.
- [17] Mendoza P A (2006). "Electronic Control of Micro-hydro plant for application in distributed generation". Available online: http://www.centroenergia.cl/literatura/memorias_tesis/memoria_Patricio_Mendoza.pdf [Accessed: 01-05-2014].
- [18] García J A, Domínguez H, Peña L, Fong J y Chang F (2004). "Perspectives automation of hydropower in Cuba". Faculty of Electrical Engineering. University of Orient, Cuba.
- [19] Abreu, A (2006). Construction of a frequency controller for a mini hydro, Diploma Work. University of Orient, Cuba.
- [20] Kurtz V, Anocibar H (2007). "Mixed control system for micro hydro generation, HIDRORED", National University of Missions, Argentina, 2007, pp 24-30. ISSN 0935-0578.
- [21] Kurtz V, Anocibar H (2007). "Alternative control ballast loads HIDRORED", National University of Missions, Argentina, 2007, pp 3-10. ISSN 0935-0578.
- [22] Kurtz V, Botero F. "An alternative for the control of ballast loads which regulate frequency and voltage in isolated operation PCH". Available online: <http://www.cerpch.unifei.edu.br/arquivos/artigos/44c1e4324ee3998d01c61875a2288b61.pdf>. [Accessed: 09-05-2014].
- [23] Fong et al (2008). "Frequency regulator for microcontroller based load ballast for micro and mini hydropower plants in operation isolated", International Conference FIE'08. 2008. Cuba. ISBN: 978-84-00-08680-0.
- [24] Dihn S (2010). "Frequency controller for micro and mini hydropower plants isolated operation", University of the Orient Headquarters Mella. Diploma work. Automatic Department. Cuba
- [25] Suárez T A (2010). "Development of a control system of frequency for a hydroelectric plant operating in isolation. Diploma work". University of the Orient. Cuba.
- [26] Peña L, Domínguez H, Fong J, García J, Alzórris P. "Frequency regulation in a Mini hydroelectric by ballast loading using a PCE Embedded". Polytechnic University of Cataluña. Available online: <http://www.aedie.org/9CHLIE-paper-send/291-PE%D1A.pdf>. [Accessed: 12-05-2014].
- [27] Vasquez H, Pinedo C, Palacios J, Ramírez J. "Frequency Regulation in Micro-hydropower by offsetting the burden". University of the Valle. Available: <http://bibliotecadigital.univalle.edu.co/bitstream/10893/1216/1/Regulacion%20de%20frecuencia%20en%20microcenrales.pdf> [Accessed: 15-05-2014].
- [28] Bory P H (2011). "Methodology for improving power factor in Small Hydro in autonomous regime and employing converters AC in CA for frequency regulation". Master's Thesis. Automatic Department. Cuba.
- [29] Bory et al (2006). "Analysis of different forms of control of single-phase rectifier bridge". FIE'06 International Conference. 2006. Cuba. ISBN: 84-00-08424-1.
- [30] Bory et al (2008). "Analysis of different forms of control phasesemiconverter", International Conference FIE'08. 2008. Cuba. ISBN: 978-84-00-08680-0.
- [31] PSIM User's Guide Version 6.0. Copyright © 2001-2003 Power sim Inc. Available online: <http://www.powersimtech.com> [Accessed: 21-05-2014].
- [32] Edson C. Bortoni, Guilherme S. Bastos, Thiago M. Abreu, Basile Kawkabani. Online Optimal Power Distribution Between Units Of A Hydro Power Plant.
- [33] Available online: [Http://www.sciencedirect.com/science/article/pii/S096014811400559X](http://www.sciencedirect.com/science/article/pii/S096014811400559X). [Accessed: 09-10-2014].

- [34] Roberto Carapellucci, Lorena Giordano, Fabio Pierguidi. Techno-economic evaluation of small-hydro power plants: Modelling and characterization of the Abruzzoregion in Italy. Available online: <http://www.sciencedirect.com/science/article/pii/S0960148114006338>. [Accessed:16-11-2014].
- [35] Pan Zhao, Jiangfeng Wang, Yiping Dai . Capacity allocation of a hybrid energy storage system for power system peak shaving at high wind power penetration level. Available online: <http://www.sciencedirect.com/science/article/pii/S0960148114006673>. [Accessed:01-12-2014].
- [36] Robert Sitzenfrei, Judith von Leon. Long-time simulation of water distribution systems for the design of small hydropower systems. Available online: <http://www.sciencedirect.com/science/article/pii/S0960148114003991>. [Accessed: 04-12-2014].
- [37] Jordan D. Kern, Dalia Patino-Echeverri, Gregory W. Characklis. An integrated reservoir-power system model for evaluating the impacts of wind integration on hydropower resources. Available online: <http://www.sciencedirect.com/science/article/pii/S0960148114003541?np=y>, [Accessed:05-12-2014].
- [38] C.P. ion, C. Marinescu. Autonomous micro hydro power plant with induction generator. Available online: http://www.researchgate.net/publication/251627439_Autonomous_micro_hydro_power_plant_with_induction_generator. [Accessed:06-12-2014].

L. A. Enríquez García. “Symmetrical Switching of a Three-Phase Rectifier to improve the power factor in the mini hydroelectric frequency control .” *IOSR Journal of Electrical and Electronics Engineering (IOSR-JEEE)*, vol. 12, no. 4, 2017, pp. 60–71.